Journal of Solid State Chemistry 184 (2011) 3008–3013

Contents lists available at SciVerse ScienceDirect

Journal of Solid State Chemistry

journal homepage: www.elsevier.com/locate/jssc

Micro- and nano-scale hollow TiO_2 fibers by coaxial electrospinning: Preparation and gas sensing

Jin Zhang, Sun-Woo Choi, Sang Sub Kim *

School of Materials Science and Engineering, Inha University, Incheon 402-751, Republic of Korea

ARTICLE INFO

Article history:
Received 9 April 2011
Received in revised form
9 September 2011
Accepted 14 September 2011
Available online 17 September 2011

Keywords:
TiO_2
Fiber
Hollow
Gas sensing

ABSTRACT

We report the preparation of micro- and nano-scale hollow TiO_2 fibers using a coaxial electrospinning technique and their gas sensing properties in terms of CO. The diameter of hollow TiO_2 fibers can be controlled from 200 nm to several micrometers by changing the viscosity of electrospinning solutions. Lower viscosities produce slim hollow nanofibers. In contrast, fat hollow microfibers are obtained in the case of higher viscosities. A simple mathematical expression is presented to predict the change in diameter of hollow TiO_2 fibers as a function of viscosity. The successful control over the diameter of hollow TiO_2 fibers is expected to bring extensive applications. To test a potential use of hollow TiO_2 fibers in chemical gas sensors, their sensing properties to CO are investigated at room temperature.

1. Introduction

In the past decade, nanosized materials have been a subject of intense research owing to their unique properties. In particular, one-dimensional (1D) nanostructured metal oxides have attracted interest due to their potential applications in many areas of technology such as optics, photonics, electronics, and biology. Among different shapes of 1D nanostructured materials, tubular structured nanomaterials such as hollow nanofibers double the surface area compared with normal nanofibers. This feature is very useful in surface-related applications such as chemical sensors or photocatalysis. Tubular structured metal oxides have already been prepared by research groups using chemical vapor deposition [1], a hydrothermal approach [2], a template method [3], and electrospinning [4].

Electrospinning is a simple and versatile method to synthesize nanofibers of various materials such as polymers, ceramics, and their composites. In most cases, it has been employed to synthesize uniform dense nanofibers [5–7]. Since Loscertales et al. first reported the successful preparation of monodispersed capsules with diameters varying between 0.15 and 10 μm via a new electrospinning set-up design using a coaxial needle [8], a number of reports on the preparation of core–shell fibers, another type of 1D nanostructure, by electrospinning have been published. Sun et al. prepared compound core–shell polymer nanofibers by applying a coaxial needle [9]. Later, Li et al. reported the first successful preparation of hollow TiO_2 nanofibers of 200–500 nm in diameter using this coaxial electrospinning method [4]. They used heavy mineral oil and a precursor solution containing Ti component as the materials for the core and shell, respectively. The oily core was extracted with octane, producing hollow fibers after a suitable calcination. Based on the coaxial electrospinning method, preparation of hollow fibers of various oxide materials including TiO_2, Fe_2O_3, $LiCoO_2$, and VO_2 has since been reported by other research groups [10–13].

Studies on the control of the diameter of hollow oxide fibers by the coaxial electrospinning are rare, in spite of the importance of this aspect in their practical applications. In this work, hollow TiO_2 fibers were prepared via an electrospinning technique with a coaxial needle. The diameters of the fibers were controlled from nano- to micro-scale by changing the viscosity of the precursor solutions. A simple mathematical expression is proposed to predict the change in diameter of the hollow TiO_2 fibers. In addition, to test their potential use in chemical gas sensors, their CO sensing properties were investigated at room temperature.

2. Experimental

Hollow TiO_2 fibers were prepared by electrospinning with a coaxial needle. Titanium isopropoxide (Aldrich) and polyvinylpyrrolidone (PVP, molecular weight ≈1,300,000, Aldrich) were used as precursor materials. As shown in Fig. 1, the coaxial electrospinning set-up consists of a high power supply, a syringe pump, an aluminum collector, two syringes, and a coaxial needle. It is basically the same as the conventional set-up except for the coaxial needle. The coaxial needle was fabricated by inserting a

* Corresponding author. Fax: +82 32 862 5546.
E-mail address: sangsub@inha.ac.kr (S.S. Kim).

0022-4596/$ - see front matter © 2011 Elsevier Inc. All rights reserved.
doi:10.1016/j.jssc.2011.09.014

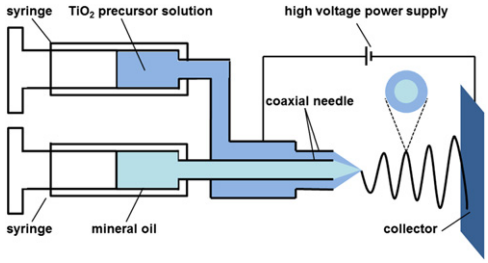

Fig. 1. Schematic illustration of the electrospinning technique with a coaxial needle used in this study.

stainless steel needle with an inner diameter of 0.5 mm and outer diameter of 0.8 mm into another stainless steel needle whose inner diameter was 1.1 mm. The inner needle was welded to the outer needle and connected to a syringe. The solutions for electrospinning were prepared as follows. First, a mixed solvent consisting of 4 ml of acetic acid (DC Chemical Co.) and 10 ml of ethanol (J. T. Baker) was prepared. Different amounts (0.8, 1.2, 1.6, and 2 g) of PVP were dissolved in the mixed solvent while stirring for 2 h at room temperature. Subsequently, 6 g of titanium isopropoxide was added to the PVP solutions, respectively, while stirring for 6 h at room temperature. In this experiment, the PVP concentration in the solutions was varied from 0.04 to 0.1 g/ml, which eventually changed the viscosity of the precursor solutions.

The prepared solution of titanium isopropoxide and PVP was loaded into a syringe connected to the outer needle. While heavy mineral oil (Aldrich), used as a core material, was loaded to another syringe connected to the inner needle. During the electrospinning process, the applied voltage was fixed at 30 kV and the feeding rate was adjusted to 0.1 ml/h. The silicon substrates placed on the aluminum collector were located 20 cm away from the tip of the needle. All the electrospinning experiments were carried out at room temperature and in an air ambient. The as-spun fibers were then immersed in octane for 12 h to remove mineral oil existing in the cores of the fibers, and subsequently dried at room temperature for 6 h. Hollow titanium isopropoxide/PVP fibers were obtained. Here, they are called "as-prepared" fibers. By calcining these hollow fibers at 600 °C for 2 h, crystalline hollow TiO_2 fibers were eventually prepared.

The viscosity of solutions was measured at room temperature using a viscometer (Brookfield Viscometer, DV-II Pro). It measures the torque required to rotate an immersed element (the spindle) in a fluid. The spindle is driven by a motor through a calibrated spring; deflection of the spring is proportional to the fluid's resistance to flow, therefore, it is also proportional to the viscosity to the fluid. The microstructure and phase of hollow TiO_2 fibers were investigated using field-emission scanning electron microscopy (FE-SEM, Hitachi/S-4200) and X-ray diffraction (XRD, Philips/X'pert MPD), respectively. Surface areas were calculated using the Brunauer–Emmett–Teller (BET) equation.

For the gas sensing measurements, Ni (~200 nm in thickness) and Au (~50 nm) double layer electrodes were sequentially deposited via sputtering on the specimens using an interdigital electrode mask. The response of the hollow TiO_2 fibers was measured at room temperature using a home-made gas dilution and sensing system in terms of CO. For comparison, a sensor was fabricated with the normal solid TiO_2 fibers using the same electrodes. The preparation procedure of the normal TiO_2 fibers are described in detail in our previous reports [7,14].

3. Results and discussion

Fig. 2 shows the microstructures of as-prepared hollow fibers, prepared with varying viscosity of solutions, obtained after being

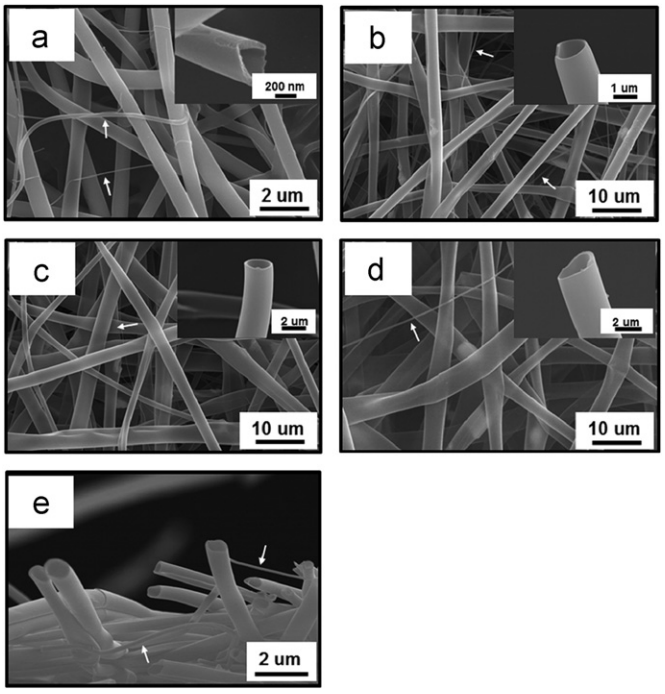

Fig. 2. SEM images of as-prepared hollow fibers with different PVP concentrations (a) 0.04, (b) 0.06, (c) 0.08, and (d) 0.1 g/ml. (e) A cross-sectional image of sample (a).

immersed in octane for 12 h. These as-prepared hollow fibers should comprise a mixture of titanium isopropoxide and PVP as well as a small amount of solvent. As shown, the microstructures of the fibers are the same in nature regardless of the PVP concentration. The semi-transparency of each fiber reveals the hollow nature of the as-prepared fibers. The inset figures are the corresponding cross-sectional images, definitely showing the successful formation of hollow fibers in the as-prepared state. Fig. 2(e) is a cross-sectional image taken from the sample of Fig. 2(a). It shows that most of the as-prepared fibers are hollow. Another thing that should be mentioned in Fig. 2 is the presence of fibers having very small diameters less than 100 nm, as indicated with white arrows. The presence of these fibers is in good agreement with the literature reported previously [4].

The average diameter of the as-prepared fibers varies depending on the content of PVP in the electrospinning solution. The variation in the concentration of PVP consequently results in a corresponding change in the viscosity of the electrospinning solution. Fig. 3(a) shows the change in viscosity as a function of PVP concentration. As expected, the viscosity increases from 142 to 867 mPa·s as the content of PVP in the precursor solution is increased. The diameter of electrospun fibers strongly depend on a number of processing parameters including the property of the electrospinning solution such as the type of polymer, the concentration of polymer, viscosity, and electrical conductivity as well as the operational conditions such as the strength of applied electric field and the feeding rate [15–18]. In our electrospinning conditions variation of the processing parameters such as the feeding rate and the applied voltage revealed no obvious effects on the diameter of the hollow fibers. However, the viscosity of the solutions played a key role in controlling the diameter of the hollow TiO_2 fibers. In general, the viscosity of a solution is related to the molecular weight and concentration of polymers dissolved in the solvent. In this study, we varied the concentration of the polymer to control the viscosity. An increase in the polymer concentration will typically result in greater entanglement of polymer chains. This is the most likely reason to explain the increase in the viscosity of the solutions.

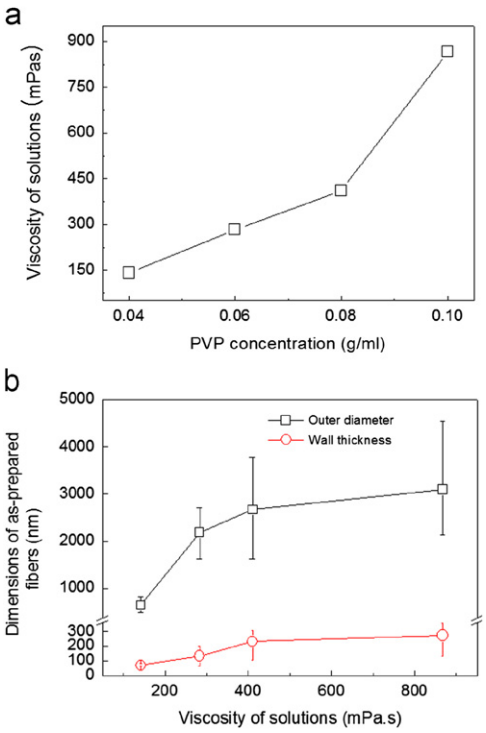

Fig. 3. (a) Change in the viscosity of the solutions as a function of PVP concentration. (b) Change in the outer diameter and wall thickness of the as-prepared hollow fibers as a function of the viscosity of the solutions.

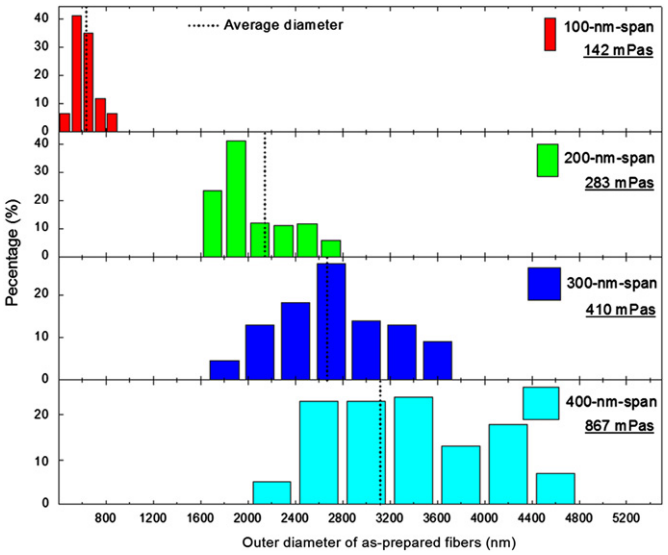

Fig. 4. A histogram of the distribution of outer diameters.

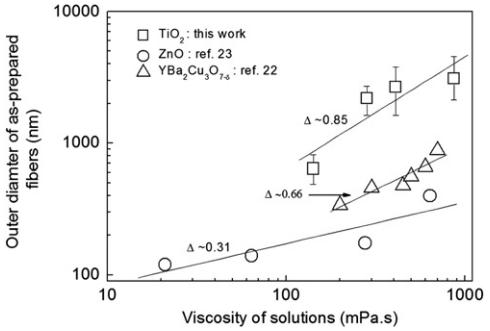

Fig. 5. Change in the outer diameter of the as-prepared hollow fibers as a function of the viscosity of the solutions (log–log plot). For comparison, the results of ZnO and $YBa_2Cu_3O_{7-\delta}$ are included.

Fig. 3(b) shows the outer diameter of the as-prepared hollow fibers before calcination as a function of the viscosity of electrospinning solution. A higher viscosity produces hollow fibers with a larger diameter in the as-prepared state. The variation of the wall thickness is included in Fig. 3(b). If we subtract the wall thickness from the outer diameter, then we can simply calculate the inner diameter of as-prepared hollow fibers. For the purpose of more clearly revealing the distribution of the outer diameter, the histogram of its distribution is provided in Fig. 4. The fibers of very small diameters were not included in the distributions because their amounts are negligible. The dotted lines indicate the average values of the outer diameters. As shown, the fibers obtained from the electrospinning solution with higher viscosities are wider in the distribution of the outer diameters.

The diameter of normal solid nanofibers of polymers is known to be related with the viscosity of electrospinning solutions, following a power law relationship [19–21]. We propose a simple mathematical expression, given as Eq. (1), to predict the relationship between the viscosity of the solutions and the diameter of oxide fibers, assuming that the diameter of the oxide fibers follows the behavior of polymer fibers

$$D - D_0 = k\eta^n \quad (1)$$

where D is the diameter of the fibers at a certain viscosity of η, D_0 is the diameter of the fibers when η approaches zero, η is the viscosity of the solution, n is an exponent, and k is a constant. When η is zero, the spinning solution usually breaks into liquid droplets, consequently generating nanoparticles instead of nanofibers. Thus, it is reasonable to neglect D_0. The plot of log D versus log η, shown in Fig. 5, readily gives the value of n. The slope n is 0.85. By extrapolating, the value of k can be obtained. Thus one can predict the outer diameter in the as-prepared state when an electrospinning solution of a particular viscosity is used. This power law relationship is quite common in electrospun polymers [19–21]. With increasing viscosity of the solution, the increased viscoelasticity usually prevents the jet segment from being stretched by the constant Coulombic force, resulting in fibers of greater diameter. It is of note that the as-prepared hollow fibers exhibit similar behavior to electrospun prepared polymer fibers in terms of variation of diameter with viscosity. In Fig. 5, for comparison, previously reported data regarding viscosity of solutions and the diameter of as-spun fibers of $YBa_2Cu_3O_{7-\delta}$ [22] and ZnO [23] are replotted in a log D–log η scheme. The linear relationships in the log D–log η plots demonstrate the validity of Eq. (1), which can be generally used to describe the change in diameter of electrospun ceramic nano or microfibers.

For the purpose of obtaining hollow fibers of pure TiO_2 phase, the as-prepared hollow fibers were calcined at 600 °C for 2 h under an air atmosphere. Fig. 6 shows typical FE-SEM images taken from the hollow TiO_2 fibers after calcination. The inset figures reveal their overall microstructures. They show that the hollow TiO_2 fibers have smooth, featureless surfaces with a well-rounded shape without any presence of grains. However, it is of note to mention that the hollow TiO_2 fibers prepared by electrospinning with a coaxial needle were composed of small grains [4]. The images displayed in Fig. 6 also suggest that the oil phase was encapsulated as a continuous, uniform thread in each fiber during the electrospinning process. Shrinkage in the diameter of the fibers due to removal of PVP and decomposition of Ti precursors during the calcination process is also evident. XRD was used to confirm the phase of the hollow TiO_2 fibers. Fig. 7 displays an XRD pattern obtained from hollow TiO_2 nanofibers prepared from the

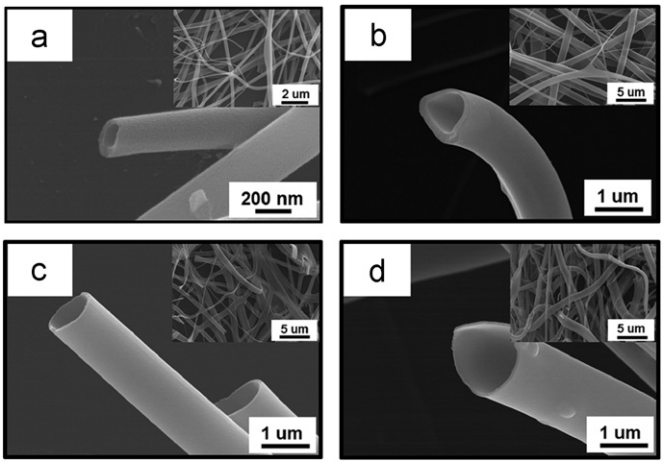

Fig. 6. FE-SEM images of TiO_2 hollow fibers obtained after calcination at 600 °C for 2 h with different PVP concentrations (a) 0.04, (b) 0.06, (c) 0.08, and (d) 0.1 g/ml. The insets are low-magnified SEM images revealing the corresponding overall morphologies of the fibers.

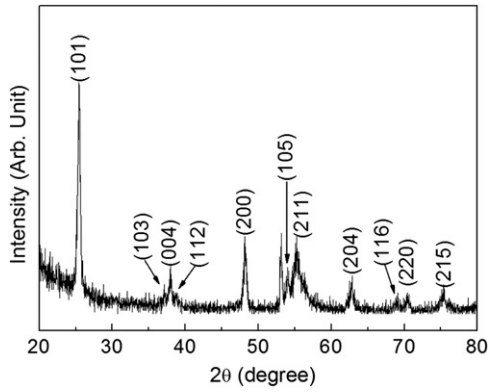

Fig. 7. Typical XRD pattern obtained from hollow TiO_2 fibers prepared from the solution with a PVP concentration of 0.04 g/ml.

solution containing 0.04 g/ml of PVP. All the peaks correspond closely with those of the pure anatase phase of TiO_2 (the JCPDS card, NO. 89-4921), indicating the hollow fibers are of anatase phase TiO_2. The XRD patterns obtained from the different samples were the same basically. The data are not presented to avoid repetition.

Fig. 8 shows the outer diameter and the wall thickness of hollow TiO_2 fibers after calcination treatment with respect to the viscosity of the electrospinning solution. The average diameter varies from 200 to 2000 nm. As expected from the results of as-prepared hollow nanofibers, the final product of hollow nanofibers is produced in the case of lower viscosities. In contrast, hollow microfibers are produced at higher viscosities. The wall thickness also gradually increases with increasing the viscosity of solutions. The inner diameter of hollow fibers can be easily calculated by subtracting the wall thickness from the outer diameter. The histogram of the distribution of the outer diameters is shown in Fig. 9. The dotted lines indicate the average values of the outer diameters. Similar to the as-prepared state, the calcined hollow fibers prepared from the electrospinning solutions with higher viscosities show wider distributions. As far as we know, no study reported to date has focused on control over the diameter of hollow oxide fibers. The successful control of the diameter of hollow TiO_2 fibers is expected to be useful for practical applications in the fields of chemical sensors and catalysis.

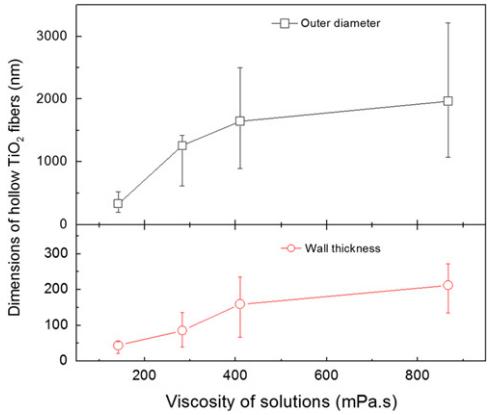

Fig. 8. Change in the outer diameter and wall thickness of the hollow TiO_2 fibers after calcination treatment as a function of the viscosity of the solutions.

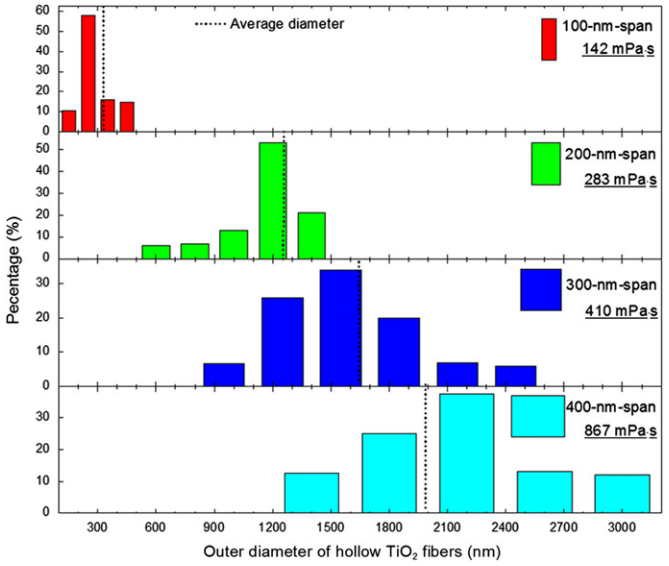

Fig. 9. A histogram of the distribution of outer diameters of the hollow TiO_2 fibers after calcination treatment.

To test the potential use of hollow TiO_2 fibers in chemical gas sensors, their CO sensing properties were investigated particularly at room temperature. A schematic diagram of the sensor fabricated with hollow TiO_2 fibers is illustrated in Fig. 10(a). The experimental set-up and procedure are described in detail in our previous reports [6,24,25]. Fig. 10(b) shows the change in resistance of the sensor fabricated with the hollow TiO_2 fibers of 200 nm in diameter at different CO concentrations ranging from 0.1 to 0.7 ppm. When the sensor is exposed to CO gas, the resistance decreases. When the CO supply is stopped, the resistance completely recovers to the initial value. This can be explained in the framework of a normal *n*-type semiconductor sensor. In the air environment before being exposed to gas molecules, oxygen molecules in the air adsorb on the surface sites of *n*-type hollow TiO_2 fibers. The adsorbed oxygen molecules attract electrons in the valence band, producing more holes in the fibers. This facilitates the conductivity along the fibers, compared with ones having a pristine surface. When the *n*-type hollow TiO_2 fibers sensor is exposed to a reducing gas such as CO, CO molecules are likely to react with the adsorbed surface oxygen, forming CO_2 molecules as $CO+O^{2-}\rightarrow CO_2+2e^-$. This liberates the extracted electrons into the holes in the valence band, consequently resulting in the suppression of conductivity.

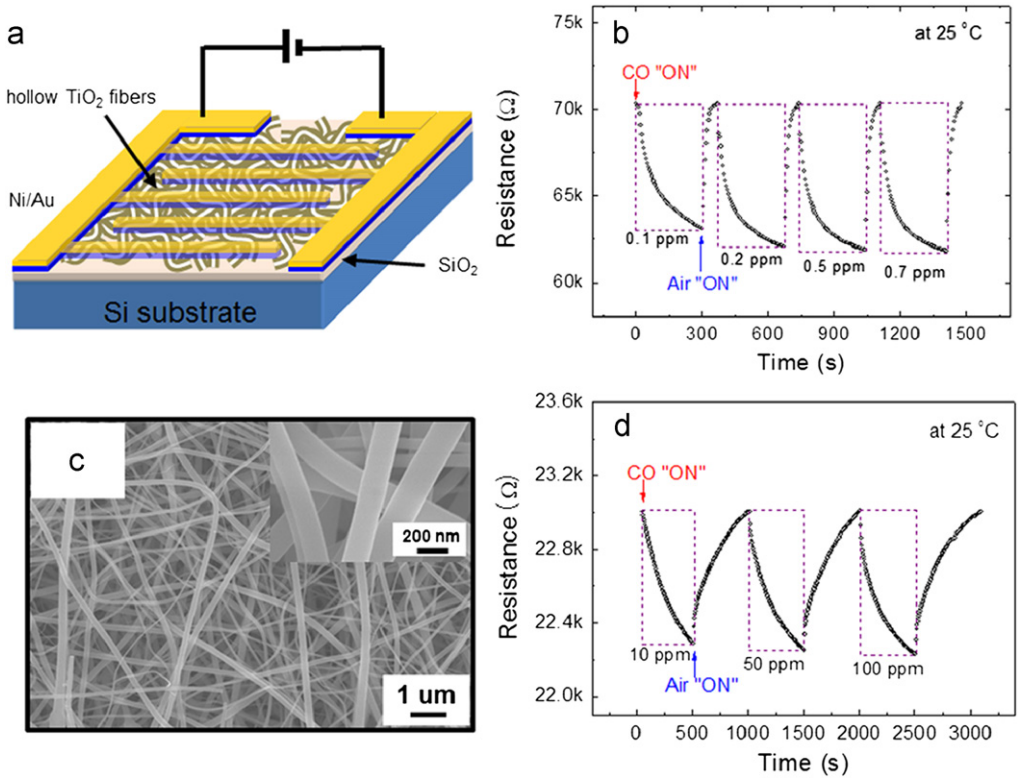

Fig. 10. (a) A schematic illustration showing the sensor fabricated with the hollow TiO_2 fibers. (b) Dynamic response at various CO concentrations for the sensor fabricated with the hollow TiO_2 fibers. (c) Microstructure of normal TiO_2 fibers. The inset figure is an enlarged image. (d) Dynamic response at various CO concentrations for the sensor fabricated with the normal TiO_2 fibers.

For comparison, the response curve of a sensor fabricated with normal TiO_2 fibers was measured. Fig. 10(c) shows the microstructure of normal TiO_2 fibers. The inset figure is an enlarged image, showing the diameter is ~200 nm. Using the normal fibers, the sensor was fabricated and its sensing properties to CO were measured. As shown in Fig. 10(d), the sensor fabricated with the normal TiO_2 fibers exhibits much inferior sensitivity to the sensor fabricated with the hollow TiO_2 fibers. Note that the sensor fabricated with the hollow TiO_2 fibers could detect CO at as low as 0.1 ppm (see Fig. 10(b)). However, no response was detected for the sensor fabricated with the normal TiO_2 fibers at 0.1 ppm CO. It is noteworthy that the CO sensing measurement was performed at room temperature. The hollow TiO_2 fibers have inner and outer surfaces, meaning that the surface-to-volume ratio almost doubles compared with normal solid nanofibers, providing much more surface adsorption sites for gas molecules. This consequently yields superior sensitivity and repeatability when hollow TiO_2 fibers are used for sensing materials. To support this claim, the surface areas of the hollow and the normal TiO_2 fibers were measured on the basis of the BET analysis. Fig. 11 shows the nitrogen adsorption–desorption isotherms of the hollow and the normal TiO_2 fibers. The BET analysis revealed that the surface area of the hollow TiO_2 fibers was 57.9 m^2/g, which was much larger than that of the normal TiO_2 fibers (22.6 m^2/g).

4. Conclusions

Hollow TiO_2 fibers were prepared via an electrospinning technique with a coaxial type needle. Importantly, the diameter of the hollow fibers changed from nano- to micro-scale in relation to the viscosity of the electrospinning solutions, which was controlled by changing the content of PVP in the solutions. As the viscosity of the solution was lowered, the diameter of the prepared hollow fibers

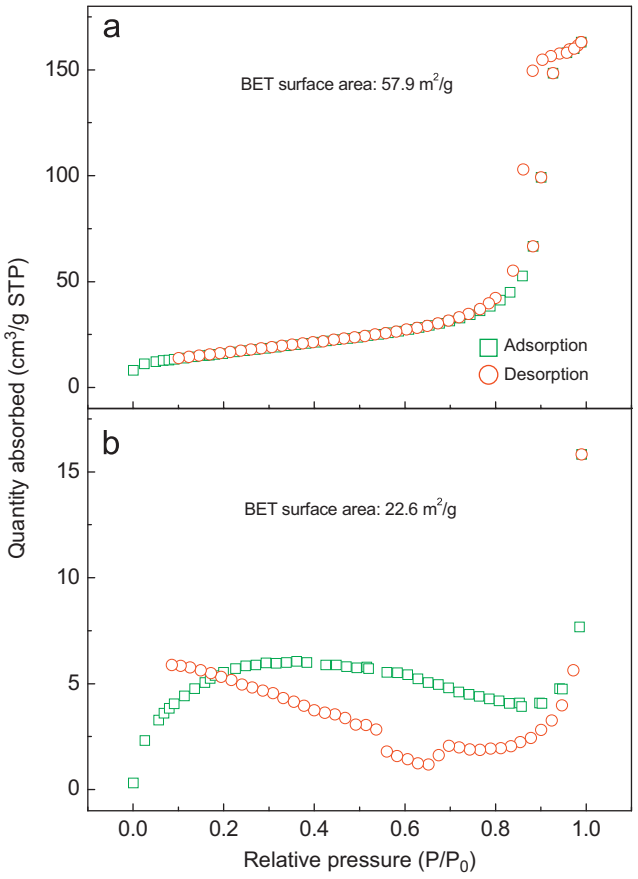

Fig. 11. Nitrogen adsorption–desorption isotherms of (a) hollow TiO_2 fibers and (b) normal TiO_2 fibers.

was accordingly decreased. The sensing properties of the hollow TiO_2 fibers with regard to CO were investigated. The clear sensing signals to CO at room temperature were observed in the hollow TiO_2 fibers due to the effect of the increase in surface-to-volume ratio by the generation of inner surfaces.

Acknowledgment

This research was supported by a grant from the Fundamental R&D Program for Core Technology of Materials funded by the Ministry of Knowledge Economy, Republic of Korea.

References

[1] B.P. Zhang, N.T. Binh, K. Wakatsuki, Y. Segawa, Y. Yamada, N. Usami, M. Kawasaki, H. Koinuma, Appl. Phys. Lett. 84 (2004) 4098–4100.
[2] B.D. Yao, Y.F. Chan, X.Y. Zhang, W.F. Zhang, Z.Y. Yang, N. Wang, Appl. Phys. Lett. 82 (2003) 281–283.
[3] L. Zhi, T. Gorelik, J. Wu, U. Kolb, K. Mullen, J. Am. Chem. Soc. 127 (2005) 12792–12793.
[4] D. Li, Y. Xia, Nano Lett. 4 (2004) 933–938.
[5] J.Y. Park, S.S. Kim, J. Am. Ceram. Soc. 92 (2009) 1691–1694.
[6] S.-W. Choi, J.Y. Park, S.S. Kim, Nanotechnology 20 (2009) 465603.
[7] J.Y. Park, S.-W. Choi, K. Asokan, S.S. Kim, J. Nanosci. Nanotechnol. 10 (2010) 3604–3608.
[8] I.G. Loscertales, A. Barrero, I. Guerrero, R. Cortijo, M. Marquez, A.M. Gañán-Calvo, Science 295 (2002) 1695–1698.
[9] Z. Sun, E. Zussman, A.L. Yarin, J.H. Wendorff, A. Greiner, Adv. Mater. 15 (2003) 1929–1932.
[10] S. Zhan, D. Chen, X. Jiao, C. Tao, J. Phys. Chem. B 110 (2006) 11199–11204.
[11] S. Zhan, D. Chen, X. Jiao, S. Liu, J. Colloid Interface Sci. 308 (2007) 265–270.
[12] S. Zhan, Y. Li, H. Yu, J. Disper. Sci. Technol. 29 (2008) 702.
[13] J.E. Panels, Y.L. Joo, J. Nanomater. (2006) 1–10.
[14] J.Y. Park, S.S. Kim, Met. Mater. Int. 15 (2009) 95–99.
[15] D.H. Reneker, I. Chun, Nanotechnology 7 (1996) 216–223.
[16] Z.-M. Huang, Y.-Z. Zhang, M. Kotaci, S. Ramakrishna, Comps. Sci. Technol. 63 (2003) 2223–2253.
[17] D. Li, Y. Xia, Adv. Mater. 16 (2004) 1151–1170.
[18] T. Subbiah, G.S. Bhat, R.W. Tock, S. Parameswaran, S.S. Ramkumar, J. Appl. Polym. Sci. 96 (2005) 557–569.
[19] P.K. Baumgarten, J. Colloid Interface Sci. 36 (1971) 71–79.
[20] M.G. McKee, G.L. Wilkes, R.H. Colby, T.E. Long, Macromolecules 37 (2004) 1760–1767.
[21] P. Gupta, C. Elkins, T.E. Long, G.L. Wilkes, Polymer 46 (2005) 4799–4810.
[22] X.M. Cui, W.S. Lyoo, W.K. Son, D.H. Park, J.H. Choy, T.S. Lee, W.H. Park, Supercond. Sci. Technol. 19 (2006) 1264–1268.
[23] D. Lin, W. Pan, H. Wu, J. Am. Ceram. Soc. 90 (2007) 71–76.
[24] J.Y. Park, S.-W. Choi, J.-W. Lee, C. Lee, S.S. Kim, J. Am. Ceram. Soc. 92 (2009) 2551–2554.
[25] J.Y. Park, S.-W. Choi, S.S. Kim, Nanotechnology 21 (2010) 475601.